

## Supporting Information

### Enhancing the peroxidase-like activity of MIL-88B by ligand exchange with polydopamine

Changzhi Hu, Yuhao Xiong, Ling Liang, Weiyuan Zuo, Fanggui Ye\* and Shulin Zhao

State Key Laboratory for the Chemistry and Molecular Engineering of Medicinal Resources, School  
of Chemistry and Pharmaceutical Science, Guangxi Normal University, Guilin, 541004, PR China

\*Corresponding author: Prof. Fanggui Ye, E-mail: fangguiye@163.com; Tel: +86-773-5856104;  
fax: +86-773-5832294

#### Contents:

- Instrument and chemicals
- Characterization
- Figure S1-S8
- Table S1-S3

## 1. Instrument and chemicals

All chemicals were of analytical grade and were used without further purification.  $\text{FeCl}_3 \cdot 6\text{H}_2\text{O}$  and dopamine (DA) were purchased from Aladdin (Shanghai, China, <http://www.aladdin-e.com>). Terephthalic acid (BDC), TMB,  $\text{H}_2\text{O}_2$ , and anhydrous sodium acetate were purchased from Shanghai Chemical Reagent Company (Shanghai, China, <https://www.sinoreagent.com>). Glucose and glucose oxidase ( $100 \text{ U mg}^{-1}$ ) were purchased from Shanghai Sangon Bioengineering Technology Service Co., Ltd. (Shanghai, China, <https://www.sangon.com>). Millipore (DI) water was produced by the Millipore purification system (Bedford, MA, USA).

## 2. Characterization

Scanning electron microscopy (SEM) was conducted with a Quanta 200 FEG SEM (Philips, Netherlands). Transmission electron microscopy (TEM) was carried out on a Tecnai F-20 electron microscope operated at 200 kV (FEI, USA). X-ray diffraction (XRD) patterns were obtained with an X' Pert PRO diffractometer (PANalytical, Netherlands) using  $\text{CuK}\alpha$  radiation. X-ray photoelectron spectroscopy (XPS) data were obtained using a Thermo ESCALAB 250XI electron spectrometer (Thermo, USA) using 150-W  $\text{AlK}\alpha$  radiation. The data of contact Angle were obtained on the dataphysics OCA15EC contact Angle measuring instrument made in Germany. Fourier transform infrared (FT-IR) spectra ( $4000\text{--}400 \text{ cm}^{-1}$ ) in KBr were recorded using a PE Spectrum One FT-IR spectrometer (PE, USA). UV absorption spectra were recorded on a model Cary 60 spectrophotometer (Agilent, USA). The Zeta potential data were obtained on the Zetasizer Nano ZS, the UK made nanoparticle particle size, Zeta potential, and molecular weight analyzer. ICP-MS is manufactured by PekinElmer for FlexAR-Nexion 300X. MALDI-TOF data is obtained on the New ultra Xtreme instrument produced by Bruker, Germany.

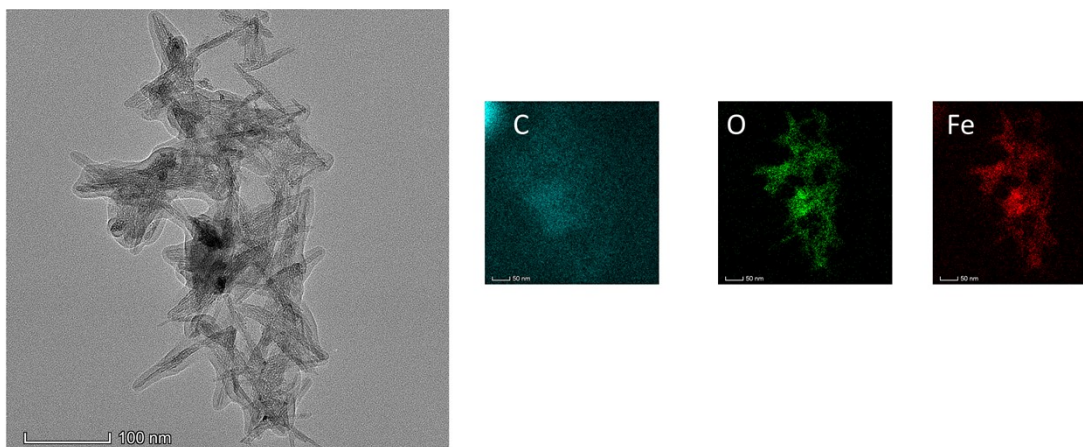


**Fig. S1** TEM images of MIL-88B and EDX mapping diagrams of C, O, Fe.

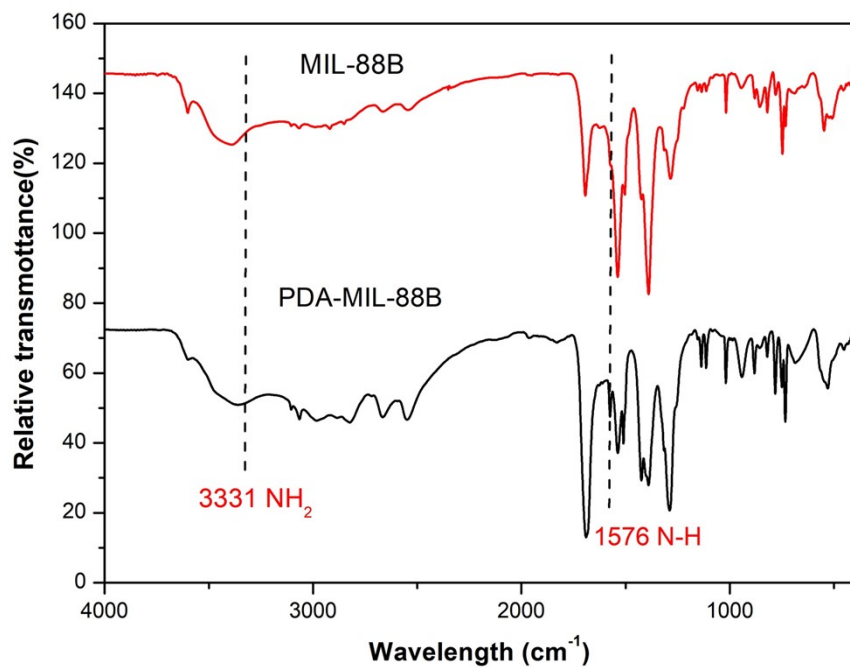


**Fig. S2** The FTIR spectra of PDA-MIL-88B and MIL-88B.

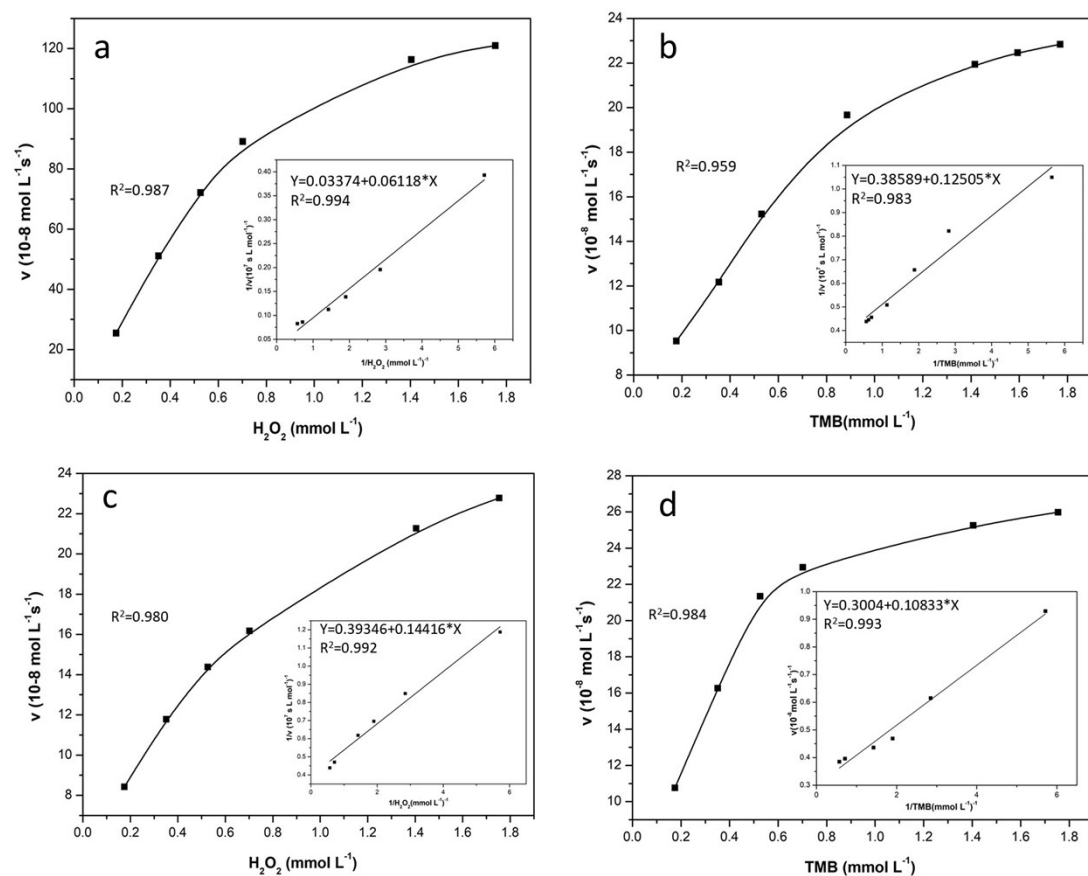


**Fig. S3** Steady-state kinetic analyses using the Michaelis-Menten model and Lineweaver-Burk model (insets) for PDA-MIL-88B by varying the concentration of  $\text{H}_2\text{O}_2$  with a fixed amount of TMB (a). Varying the concentration of TMB with a fixed amount of  $\text{H}_2\text{O}_2$  (b). Steady-state kinetic analyses using the Michaelis-Menten model and Lineweaver-Burk model (insets) for MIL-88B by varying the concentration of  $\text{H}_2\text{O}_2$  with a fixed amount of TMB (c). Varying the concentration of TMB with a fixed amount of  $\text{H}_2\text{O}_2$  (d).

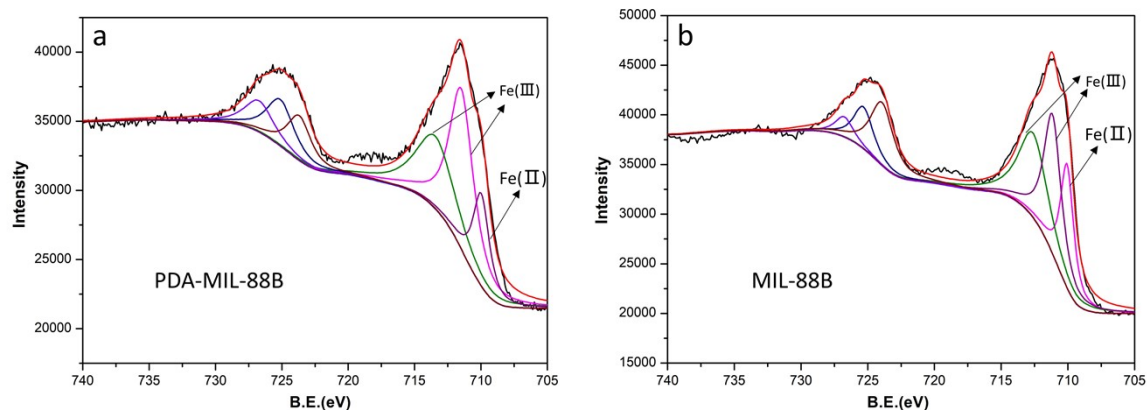


**Fig. S4** XPS spectra of PDA-MIL-88B (a) and MIL-88B (b). The table contains the proportion of elements C, Fe, and N of MIL-88B and PDA-MIL-88B.

**PDA-MIL-88B:**

Name	Start BE	Peak BE	End BE	Height CPS	FWHM eV	Area(P) CPS.eV	Area (N) TPP-2M	Atomic %
C1s	298.57	284.8	279.77	100889.63	1.45	211924.76	2971.69	89.91
Fe2p	740.57	711.47	700.77	15833.08	5	146213.07	198.93	6.02
N1s	410.57	400.27	392.77	4189	2.88	14889.22	134.59	4.07

**MIL-88B:**

Name	Start BE	Peak BE	End BE	Height CPS	FWHM eV	Area(P) CPS.eV	Area (N) TPP-2M	Atomic %
C1s	298.51	284.8	279.71	90814.18	1.38	175385.44	2459.32	89.29
Fe2p	740.51	711.08	700.71	22439.64	4.18	193419.33	263.05	9.55
N1s	410.51	399.9	392.71	874.71	1.62	3547.09	32.05	1.16

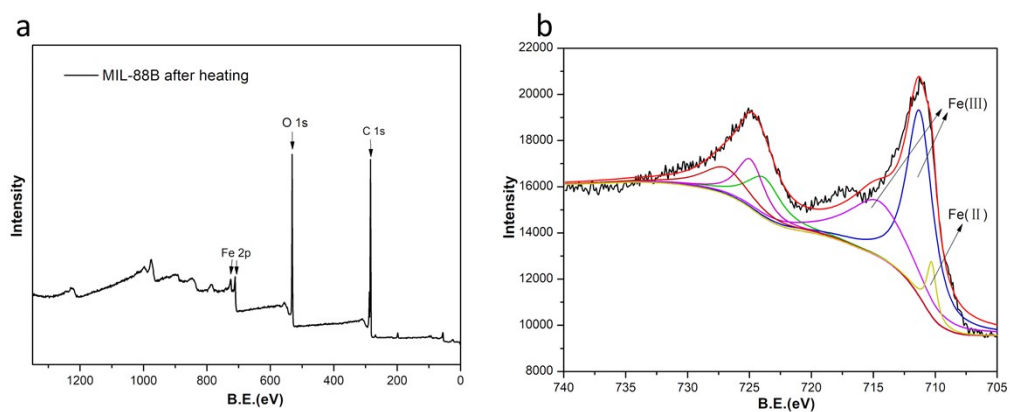


**Fig. S5** XPS spectra of MIL-88B after heating (a); XPS of Fe in MIL-88B after heating (b).

Corresponding peak area data:

Peak	Position	Area	FWHM	%GL
0	606.046eV	0.100	15.574eV	80%
1	723.816eV	8677.088	3.393eV	80%
2	711.252eV	30089.920	2.533eV	80%
3	714.574eV	20824.520	5.875eV	80%
4	724.910eV	8319.177	2.677eV	80%
5	726.947eV	7315.471	4.308eV	80%
6	710.292eV	3161.209	0.907eV	80%

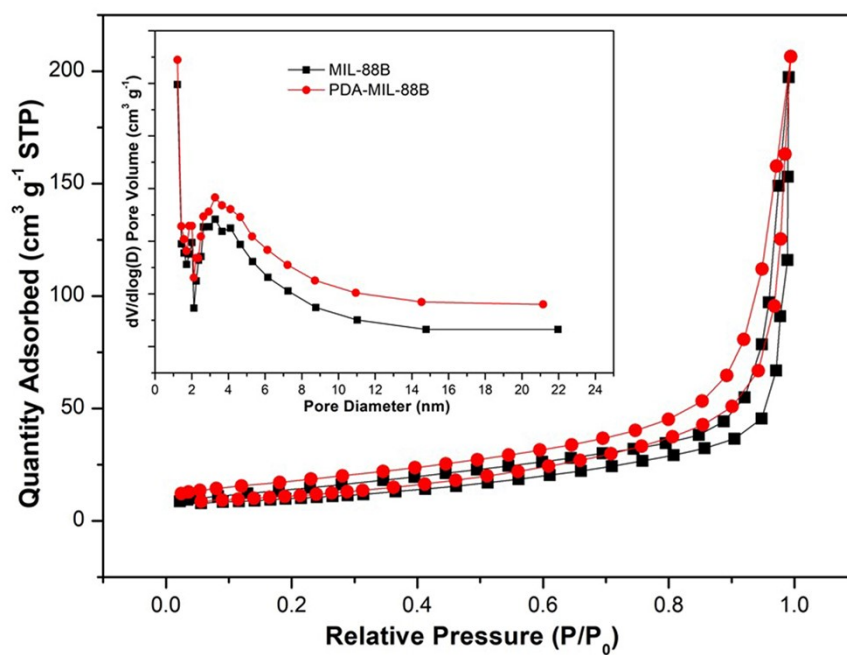


**Fig. S6** N<sub>2</sub> adsorption-desorption curves of MIL-88B and PDA-MIL-88B (inset shows the pore size distribution curves of MIL-88B and PDA-MIL-88B).

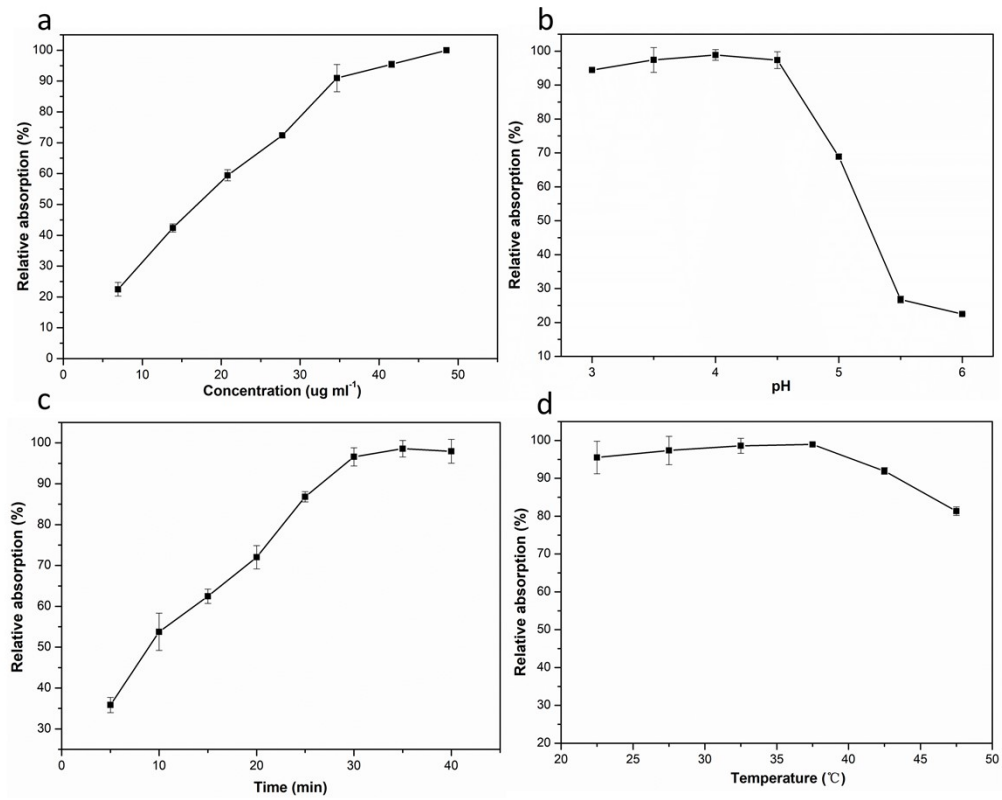


**Fig. S7** Optimization of experimental conditions.

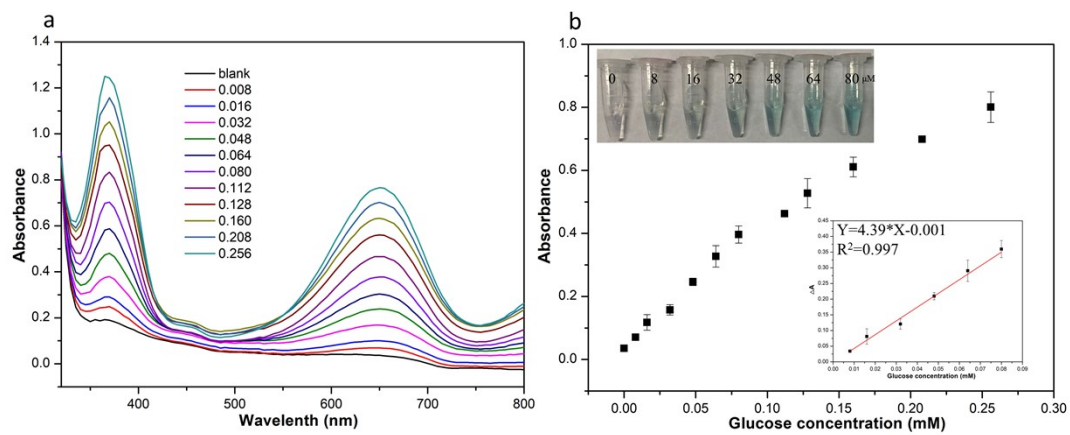


**Fig. S8** After adding different concentrations of glucose, the UV-visible absorbance at 650 nm changes (a). The variation trend of absorbance with glucose concentration and the linear fitting line between absorbance and glucose concentration (insets) (b).

**Table S1** A comparison of different nanozymes materials for detection of H<sub>2</sub>O<sub>2</sub> and glucose

Materials	Method	Linear range of	Linear range of	Reference
		H <sub>2</sub> O <sub>2</sub> / Limit of detection (μM)	glucose/ Limit of detection (μM)	
Fe-CDs	Colorimetry	6-42 /0.93	10-70 /1.73	[1]
PDI-Co <sub>3</sub> O <sub>4</sub>	Colorimetry	3-60/2.37	5-100 /2.77	[2]
Au@TiO <sub>2</sub>	Colorimetry	5-100/4.00	0-10 /3.5	[3]
CQDs	Colorimetry	5-60/0.86	10-200/2.89	[4]
Fe-CDs	Fluorescence	0-133/0.47	0-300/2.5	[5]
UCNPs	Fluorescence	2.5-70/0.8	7-110/2.3	[6]
CQDs/Cu <sub>2</sub> O	Electrochemistry	5-5300/2.8	20-4300/8.4	[7]
PDA-MIL-88B	Colorimetry	2.2-52.8/0.6	4.4-52.8/1.1	This work

[1] R. Bandi, M. Alle, C. W. Park, S. Y. Han, G. J. Kwon, N. H. Kim, J. C. Kim and S. H. Lee. *Sensors and Actuators B: Chemical*, 2021, 330, 129330.

[2] Y. Ding, M. Chen, K. Wu, M. Chen, L. Sun, Z. Liu, Z. Shi and Q. Liu. *Materials Science and Engineering: C*, 2017, 80, 558-565.

[3] X. Peng, G. Wan, L. Wu, M. Zeng, S. Lin and G. Wang. *Sensors and Actuators B: Chemical*, 2018, 257, 166-177.

[4] C. Yuan, X. Qin, Y. Y. Xu, Q. Jing, R. Shi and Y. Wang. *Microchemical Journal*, 2020, 159, 105365.

[5] D. Zhu, S. Zhuo, C. Zhu, P. Zhang and W. Shen. *Analytical Methods*, 2019, 11, 2663-2668.

[6] H. Chen, A. Fang, L. He, Y. Zhang and S. Yao. *Talanta*, 2017, 164, 580-587.

[7] Y. Li, Y. Zhong, Y. Zhang, W. Weng and S. Li. *Sensors and Actuators B: Chemical*, 2015, 206, 735-743.

**Table S2** Comparison of traditional enzymatic method and colorimetric method for determination of glucose in human serum

Sample	glucose content by conventional enzymatic <sup>a</sup> method (mM)	Glucose content by colorimetric method (mM) Mean <sup>b</sup> ± SD <sup>c</sup>	relative error (%)	RSD (%)
Sample 1	5.07	5.23±0.10	+3.1	1.9
Sample 2	4.85	4.80±0.04	-1.0	0.8
Sample 3	5.00	5.19±0.13	+3.7	2.5
Sample 4	4.81	4.77±0.05	-0.8	1.0
Sample 5	5.48	5.72±0.21	+4.2	3.4
Sample 6	5.77	5.75±0.06	-0.3	1.1

a: The data comes from the hospital report;

b: n = 3;

c: SD: Standard Deviation

Sample	Original ( $\mu\text{M}$ )	Added ( $\mu\text{M}$ )	Found ( $\mu\text{M}$ )	Recovery (%)	RSD (%)
		4.4	21.10 $\pm$ 0.50	97.72	2.4
Sample 2	16.8	8.8	26.06 $\pm$ 0.82	105.2	3.2
		16.7	33.39 $\pm$ 0.44	99.34	1.4
Sample 3	17.5	8.8	26.10 $\pm$ 0.23	97.73	1.3
		16.7	35.82 $\pm$ 1.10	109.7	1.8
		26.3	46.31 $\pm$ 0.14	108.4	0.6

**Table S3** The recovery test of our assay for detecting glucose in human serum.